Proton Nuclear Magnetic Resonance Sequential Assignments and Secondary Structure of an Immunoglobulin Light Chain-Binding Domain of Protein L†

Mats Wikström,*,‡ Ulf Sjöbring,§ William Kastern,‖ Lars Björck,⊥ Torbjörn Drakenberg,‡,▽ and Sture Forsén*,‡

Departments of Physical Chemistry 2, Medical Microbiology, and Medical and Physiological Chemistry, University of Lund, Lund, Sweden, Chemical Laboratory, Technical Research Centre of Finland (VTT), Espoo, Finland, and Department of Pathology, College of Medicine, University of Florida, Gainesville, Florida 32610

Received November 4, 1992

ABSTRACT: The ^{1}H NMR assignments have been made for the immunoglobulin (Ig) light chain-binding B1 domain of protein L from *Peptostreptococcus magnus*. The secondary structure elements and the global folding pattern were determined from nuclear Overhauser effects, backbone coupling constants, and slowly exchanging amide protons. The B1 domain was found to be folded into a globular unit of 61 amino acid residues, preceded by a 15 amino acid long disordered N-terminus. The folded portion of the molecule contains a four-stranded β-sheet spanned by a central α-helix. The fold is similar to the IgG-binding domains of streptococcal protein G, despite the fact that the binding sites on immunoglobulins for the two proteins are different; protein G binds IgG through the constant (Fc) part of the heavy chain, whereas protein L has affinity for the variable domain of Ig light chains.

Several immunoglobulin- (Ig-)[1] binding microbial proteins have been identified and isolated [for references see Boyle (1990)], the two most well-known being protein A of *Staphylococcus aureus* (Forsgren & Sjöquist, 1966), and protein G of group C and G streptococci (Reis et al., 1984; Björck & Kronvall, 1984). Among these various proteins, only protein L binds Ig through interactions with Ig light chains. This protein is expressed on the surface of some strains of the anaerobic bacterial species *Peptostreptococcus magnus* (Myhre & Erntell, 1985). It was originally isolated from the bacteria after solubilization with proteolytic and muranolytic enzymes (Björck, 1988). Protein L is an elongated, fibrous molecule (Åkerström & Björck, 1989) showing affinity for framework structures in the variable domain of κ light chains (Nilson et al., 1992). In contrast to other Ig-binding bacterial proteins, protein L appears to be a virulence determinant. Thus, protein L-expressing strains of *P. magnus* are more frequently associated with clinical infections as compared to strains that do not have the protein L gene (Kastern et al., 1990). The primary structure of protein L was recently determined, and the Ig light chain-binding activity was located to five homologous domains (B1–B5), each comprising 72–76 amino acid residues (Kastern et al., 1992). The organization of the entire protein L molecule is schematically shown in Figure 1. In this paper, we present the ^{1}H NMR sequence-specific resonance assignments, the secondary structure, and the global fold for the immunoglobulin light chain-binding B1 domain of protein L.

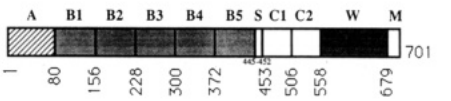

FIGURE 1: Schematic representation of protein L. The mature protein consists of 701 amino acid residues. Amino acid numbers of the beginning of each domain are listed below the boxes. Included are the N-terminal domain (A), the repeated Ig light chain-binding domains (B), the short spacer region (S), the twin repeats (C) of unknown function, the wall-spanning domain (W), and the transmembrane region (M).

MATERIALS AND METHODS

Protein Production. The first (B1) of the five highly homologous Ig light chain-binding domains of protein L was expressed in *Escherichia coli* with some modifications to the protocol previously described in Kastern et al. (1992). Briefly, a polymerase chain reaction generated DNA fragment covering the sequence encoding the 76 amino acids of the B1 domain, as well as the two C-terminal residues (EN) of the A domain of protein L was cloned into the secretion vector pHD389 (Dalböge et al., 1989). DNA inserted into the unique *Nar*I site of pHD389 cotranslates with the signal sequence (21 amino acids) of *E. coli* outer membrane protein A (*ompA*). The construct allowed secretion of the expressed peptide into the periplasmic space of the bacterium. A unique methionine was introduced between the C-terminal residue of the signal sequence and the N-terminal amino acid of the protein L-derived sequence, enabling CNBr cleavage of Ig-binding peptides that contain an unprocessed signal sequence. Periplasmic proteins were recovered by osmotic shock from *E. coli* which had been transformed with the construct, and Ig-

† This work was supported by grants from the Swedish Medical Research Council (Projects 10434 and 09926), and the Swedish Research Council for Engineering Sciences (Project 123). The 500-MHz NMR spectrometer was purchased with grants from the Knut and Alice Wallenberg Foundation and the Swedish Council for Planning and Coordination of Research. T.D. acknowledges the NESTE Foundation for a NESTE visiting scientist scholarship. M.W. acknowledges grants from the Royal Physiographical Society in Lund.

* Corresponding authors: Physical Chemistry 2, Chemical Center, P.O. Box 124, S-221 00 Lund, Sweden.

‡ Department of Physical Chemistry 2, University of Lund.

§ Department of Medical Microbiology, University of Lund.

‖ Department of Pathology, University of Florida.

⊥ Department of Medical and Physiological Chemistry.

▽ Chemical Laboratory, VTT.

[1] Abbreviations: Ig, immunoglobulin; NMR, nuclear magnetic resonance; 2D, two-dimensional; NOE, nuclear Overhauser enhancement; NOESY, nuclear Overhauser enhancement spectroscopy; COSY, *J*-correlated spectroscopy; TOCSY, total correlation spectroscopy; DIPSI, decoupling in the presence of scalar interactions; 2Q, double quantum; 2QF-COSY, double-quantum-filtered COSY; R-COSY, relayed COSY; $d_{NN}(i,j)$, NOE connectivity between the NH proton on residue i and the NH proton on residue j; $d_{\alpha N}(i,j)$, NOE connectivity between the αCH proton on residue i and the NH proton on residue j; $d_{\beta N}(i,j)$, NOE connectivity between the βCH proton on residue i and the NH proton on residue j; $d_{\alpha\alpha}(i,j)$, NOE connectivity between the αCH proton on residue i and the αCH proton on residue j.

0006-2960/93/0432-3381$04.00/0 © 1993 American Chemical Society

binding peptides were then purified from the shock lysate by affinity chromatography on IgG–Sepharose 4B (Pharmacia) (Björck, 1988).

The affinity-purified peptides were subsequently cleaved with CNBr, in 100-fold molar excess relative to methionine, in 70% formic acid at 37 °C for 16 h. The acid was removed using a Rotavapor evaporator, and the protein was solubilized in 20 mM Tris-HCl buffer, followed by dialysis against 20 mM Tris-HCl, pH 7.5. The final purification was performed on Mono Q HR5/5 or HR10/10 columns (Pharmacia LKB, Uppsala, Sweden), using a NaCl gradient from 0.1 to 0.2 M in 20 mM Tris-HCl, pH 7.5. The fractions containing the B1 domain were pooled, dialyzed extensively against water, and lyophilized. The material appeared as a single band upon analysis by sodium dodecyl sulfate–polyacrylamide (18% total acrylamide) and agarose gel electrophoresis. A previously described competitive binding assay was used to confirm the binding activity of the peptide (Akerström & Björck, 1989). Sequence determination of the five N-terminal amino acids revealed the correct sequence (ENKEE), and quantitative amino acid analysis of the entire protein gave the expected amino acid composition.

NMR Experiments. The protein samples were dissolved in 0.70 mL of H_2O containing 0.02% NaN_3 and 10% D_2O, for the lock signal, or in 99.95% D_2O with 0.02% NaN_3, resulting in a protein concentration of 3–4 mM. The pH was adjusted to 5.0 or 6.0 without correcting for isotopic effects. The NMR experiments were performed either on a GE Ω 500 spectrometer operating at 500.13 MHz or a Varian Unity 600 NMR spectrometer operating at 599.95 MHz. Data were acquired at two temperatures, 27 and 37 °C.

Standard pulse sequences were used to obtain phase-sensitive hypercomplex COSY (Aue et al., 1976; States et al., 1982), R-COSY (Wagner, 1983) in H_2O with a 30-ms mixing time, and 2QF-COSY (Rance et al., 1983) in D_2O. 2Q experiments were performed as described by Braunschweiler et al. (1983) and Levitt and Freeman (1979) with a mixing time of 30 ms. TOCSY experiments (Braunschweiler & Ernst, 1983; Bax & Davis, 1985) were performed using the modifications suggested by Rance (1987) with the DIPSI-2 mixing sequence (Shaka et al., 1988), and mixing times of 80 and 120 ms. NOESY spectra (Macura & Ernst, 1980), were acquired using a composite read pulse as described by Bax (1985), with several mixing times ranging from 40 ms up to 200 ms. The carrier was set on the solvent resonance for all experiments. Preacquisition delays of 1.1–1.3 s were used and a total of 512 spectra were collected, each with 2048 complex points. Sixty-four scans were acquired for each spectrum. The spectral widths were 5555 and 7000 Hz at 500 and 600 MHz, respectively. Solvent suppression was achieved by presaturation of the water signal during the preacquisition delay in the experiments performed in H_2O. No presaturation was applied for experiments in D_2O. The raw data were transformed with the Ω or Unity software on SUN 3/260 or Sparc II workstations. Phase-shifted squared sine-bell window functions were applied in both dimensions to the data sets that were cosine-modulated in the ω_1 dimension. For sine-modulated data, an unshifted sine-bell was used. The final 2D spectra were typically 1024 × 2048 complex points after zero-filling in the evolution dimension. After transformation, the data were analyzed using our in-house software MAGNE. In the TOCSY and NOESY experiments, the baselines were flattened using a dispersive fit (Adler & Wagner, 1991), in the MAGNE suite of programs.

Slowly exchanging amide protons were identified in a 15-h COSY experiment initiated 1 h after dissolution of the protein in D_2O at pH 5.0 and 27 °C.

Backbone $^3J_{HN\alpha}$ coupling constants were measured from a COSY spectrum in H_2O zero-filled to 1024 × 4096 points (digital resolution in ω_2 1.4 Hz/point) at pH 6.0 and 27 °C. This was done within MAGNE, by performing a least-squares fit of two Lorenztian antiphase lines to the NH/H^α cross peaks. The program reports the coupling constant, in hertz, as the shift difference between those lines.

RESULTS

The numbering of the amino acids of the studied peptide is as in the intact protein, with Glu78 from the A domain as the first residue. The B1 domain starts with Lys80.

Spin System Assignments. The ^1H NMR resonance assignments followed the procedure outlined by Wüthrich (1986), in combination with the strategy described in Chazin et al. (1988) using the interactive MAGNE program. This approach relies on the observation of scalar connectivities from the amide protons to side-chain protons in H_2O. To resolve ambiguities and to be able to observe resonances saturated by the water presaturation, four data sets were acquired at 27 and 37 °C and pH 5.0 and 6.0. The same set of connectivities was observed under the different experimental conditions, indicating no conformational changes. By using direct or relayed connectivities observed in COSY, 2Q, R-COSY, and TOCSY experiments acquired in H_2O it was possible to identify the majority of the spin systems. To completely assign the long side chains, experiments recorded in D_2O were used.

2Q spectra were used for the identification of the five glycines from their characteristic remote peaks. The spin systems of the nine alanine, three serine, and 11 threonine residues were identified using the R-COSY and TOCSY experiments. The resonances of the three valines, three isoleucines, and three leucines were assigned using COSY and TOCSY spectra in H_2O and the 2QF-COSY in D_2O. The spin systems for the aromatic residues, four tyrosines and four phenylalanines, were identified from COSY and TOCSY spectra in H_2O and by the observation of cross peaks between the ring protons and the corresponding βCH protons in a 200-ms NOESY spectrum in D_2O. The βCH_2 and γCH_2 resonances of 11 out of 12 Glu residues and the single Gln residue were assigned using TOCSY spectra. No resonances could unambiguously be assigned to the N-terminal Glu residue because of severe spectral overlap in the aliphatic region among the 12 Glu residues. TOCSY spectra were used for the assignment of the five Asp and four of the five Asn residues. No NH resonance was identified for the second residue in the protein, Asn79 from the A domain. This resonance is probably attenuated by saturation transfer effects from the saturated water due to sufficiently fast amide proton–solvent exchange. The resonances of Asn79 were found as the remaining spin system after all others were assigned. The eight Lys residues were assigned by a combination of COSY and TOCSY in H_2O and 2QF-COSY in D_2O. Finally, the shifts for the two proline residues were obtained from COSY and TOCSY experiments, and by using sequential $d_{\alpha N}(i, i+1)$ connectivities in the NOESY experiments.

Sequential Assignments. The sequence-specific assignments were obtained using the procedure of Billeter et al. (1982). The assignments were based on NOESY spectra in H_2O and D_2O with 200 ms mixing times. Sequential connectivities were observed throughout the polypeptide backbone. The complete ^1H NMR assignments are given in Table I. Figure 2A shows part of a NOESY spectrum, with

Table I: ^{1}H NMR Chemical Shifts (ppm) for the B1 Domain of Protein L at 27 °C and pH 6.0[a]

residue	NH	αCH	βCH	others
E78[b]				
N79		4.78	2.88, 2.77	δNH_2 7.65, 6.91
K80	8.57	4.37	1.89, 1.80	γCH_2 1.45; δCH_2 1.75; ϵCH_2 3.01
E81	8.48	4.32	2.08, 1.98	γCH_2 2.30
E82	8.41	4.38	2.08, 1.96	γCH_2 2.28
T83	8.31	4.65	4.19	γCH_3 1.27
P84		4.47	2.32, 1.94	γCH_2 2.02; δCH_2 3.86, 3.75
E85	8.54	4.33	2.06, 1.97	γCH_2 2.25
T86	8.28	4.63	4.19	γCH_3 1.27
P87		4.45	2.34, 1.92	γCH_2 2.02; δCH_2 3.86, 3.75
E88	8.60	4.36	2.11, 2.00	γCH_2 2.34
T89	8.18	4.40	4.25	γCH_3 1.22
D90	8.42	4.68	2.79, 2.73	
S91	8.33	4.50	3.94, 3.88	
E92	8.50	4.41	2.16, 1.99	γCH_2 2.38
E93	8.33	4.26	2.10, 2.01	γCH_2 2.34
E94	8.37	4.22	2.11, 1.95	γCH_2 2.25
V95	9.13	4.77	2.48	γCH_3 1.14, 0.95
T96	8.11	5.06	3.92	γCH_3 1.04
I97	9.36	4.79	1.87	γCH_2 1.26, 1.10; γCH_3 0.69; δCH_3 0.44
K98	8.73	4.84	1.92	γCH_2 1.48, 1.33; δCH_2 1.75; ϵCH_2 3.01
A99	9.31	5.48	1.36	
N100	9.19	5.18	3.20, 2.53	δNH_2 7.58, 6.78
L101	9.36	4.94	1.87	γH 1.76; δCH_3 1.04, 0.93
I102	9.06	4.44	1.71	γCH_2 0.95, 1.41; γCH_3 1.02; δCH_3 0.78
F103	8.59	4.94	3.37, 3.08	δCH 7.00; ϵCH 6.67; ζCH 6.91
A104	9.28	4.27	1.52	
N105	7.97	4.68	3.35, 2.91	δNH_2 7.66, 6.98
G106	8.34	4.40, 3.73		
S107	8.00	4.63	4.14, 4.05	
T108	8.32	5.73	4.16	γCH_3 1.19
Q109	9.10	4.82	2.31, 2.22	γCH_2 2.57, 2.50; ϵNH_2 7.52, 6.79
T110	8.78	5.55	4.05	γCH_3 1.26
A111	9.21	4.60	1.14	
E112	7.94	5.16	1.95, 1.70	γCH_2 2.10
F113	8.96	4.61	3.16, 2.60	δCH 7.10; ϵCH 6.95; ζCH 6.63
K114	8.79	5.70	1.77, 1.63	γCH_2 1.31, 1.48; δCH_2 1.61; ϵCH_2 2.89
G115	8.52	4.22, 4.16		
T116	8.06	4.78	4.37	γCH_3 1.42
F117	9.52	3.78	3.22, 3.11	δCH 6.96; ϵCH 6.78; ζCH 7.10
E118	9.20	3.99	2.16, 2.03	γCH_2 2.41
K119	7.64	4.07	1.94	γCH_2 1.52; δCH_2 1.79; ϵCH_2 3.07
A120	9.18	3.99	1.04	
T121	7.54	3.41	3.97	γCH_3 1.11
S122	7.66	4.21	4.03	
E123	8.29	3.94	2.33, 2.11	γCH_2 2.57
A124	7.44	2.67	0.80	
Y125	7.58	3.97	3.11, 2.78	δCH 7.26; ϵCH 6.67
A126	8.14	4.22	1.53	
Y127	8.13	4.47	3.32, 3.11	δCH 7.16; ϵCH 6.86
A128	8.27	3.77	0.89	
D129	8.73	4.87	3.09, 2.75	
T130	7.95	4.27	4.39	γCH_3 1.51
L131	7.62	4.42	2.12	γH 1.41; δCH_3 1.08, 0.68
K132	7.87	4.82	2.11, 2.05	γCH_2 1.52; δCH_2 1.92; ϵCH_2 3.05
K133	7.93	4.02	1.91	γCH_2 1.49; δCH_2 1.75; ϵCH_2 3.06
D134	7.63	4.87	2.64, 2.36	
N135	7.84	4.94	2.54, 2.16	δNH_2 7.41, 7.25
G136	8.49	4.52, 3.92		
E137	8.05	4.07	2.04, 1.85	γCH_2 2.39, 2.28
Y138	7.72	5.72	2.02, 1.47	δCH 6.52; ϵCH 6.64
T139	8.43	4.58	4.20	γCH_3 1.20
V140	8.65	4.87	2.07	γCH_3 1.00, 0.90
D141	9.02	5.08	2.78, 2.70	
V142	8.68	4.30	2.06	γCH_3 0.99
A143	9.32	4.95	1.36	
D144	9.13	4.44	2.94, 2.84	
K145	8.99	3.88	2.18	γCH_2 1.49; δCH_2 1.78; ϵCH_2 3.06
G146	7.68	4.56, 3.44		
Y147	7.72	4.59	3.60, 3.13	δCH 7.54; ϵCH 6.84
T148	7.80	5.30	3.71	γCH_3 1.04
L149	9.18	4.76	1.60	γH 1.42; δCH_3 0.47, 0.81
N150	8.77	5.44	3.13, 2.45	δNH_2 7.31, 6.98
I151	9.33	4.46	1.72	γCH_2 1.36, 0.62; γCH_3 −0.04; δCH_3 0.37
K152	8.50	5.12	1.77, 1.57	γCH_2 1.26; δCH_2 1.62; ϵCH_2 2.92
F153	8.87	4.79	3.48, 3.09	δCH 7.16; ϵCH 6.98; ζCH 6.92
A154	9.02	4.39	1.60	
G155	8.26	3.97, 3.63		

[a] Chemical shifts are referenced to the H_2O signal at 4.75 ppm and are accurate to ±0.02 ppm. [b] Signals from this residue were not detected.

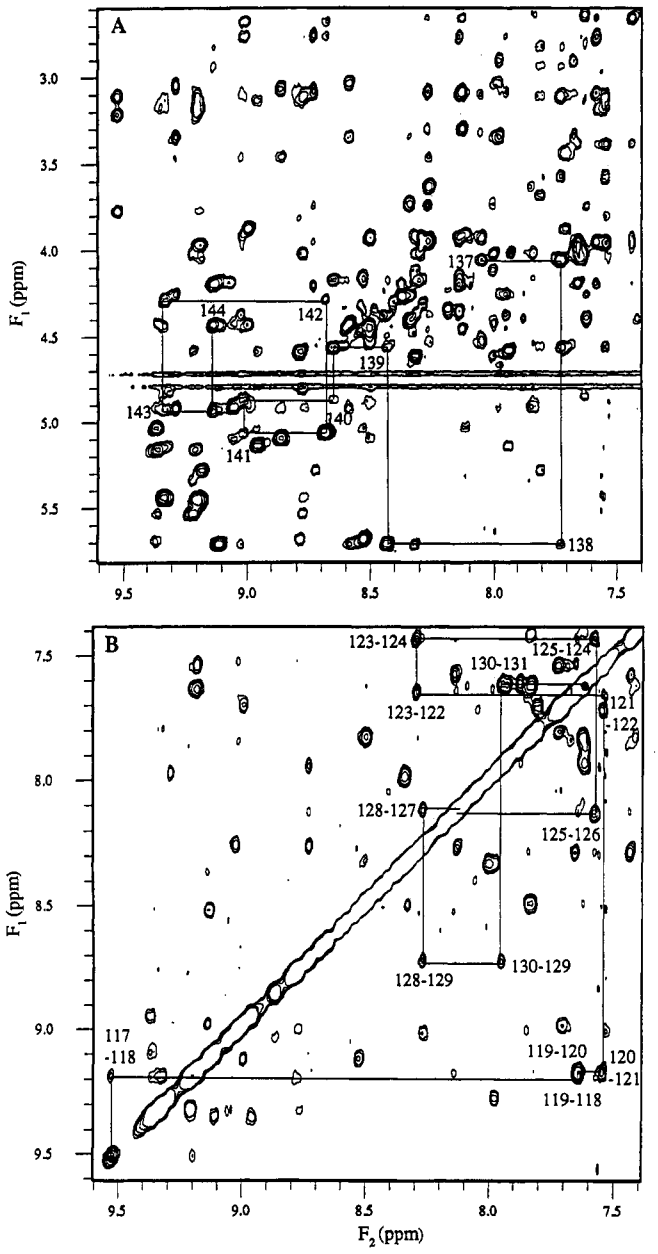

FIGURE 2: Selected regions of a NOESY spectrum of the B1 domain in H_2O, at 27 °C and pH 6.0, showing in panel A $d_{\alpha N}(i, i + 1)$ connectivities for residues Glu137–Asp144 (the intraresidue $d_{\alpha N}$ connectivities are numbered), and in panel B $d_{NN}(i, i + 1)$ connectivities for residues Phe117–Leu131 (residue number in F_2-residue number in F_1).

the sequential $d_{\alpha N}(i, i + 1)$ connectivities traced for residues Glu137–Asp144. Figure 2B shows the sequential $d_{NN}(i, i + 1)$ connectivities for residues Phe117–Leu131. A summary of the sequential and medium-range connectivities observed in the B1 domain is shown in Figure 3.

Secondary Structure. The first 15 residues of the B1 domain showed only short-range connectivities and fast amide proton exchange. The resonances from these residues were also significantly more narrow than signals from other residues, suggesting a higher mobility. Thus, the N-terminus appears to be disordered and most likely not involved in the global fold of the molecule.

A four-stranded β-sheet platform was identified by the observation of interstrand $d_{NN}(i,j)$, $d_{\alpha N}(i,j)$, and $d_{\alpha\alpha}(i,j)$ connectivities, shown in Figure 4. These connectivities show that β-strands $\beta1$ (Val95–Phe103) and $\beta2$ (Ser107–Gly115) are antiparallel. Another antiparallel pair of β-strands is formed by $\beta3$ (Glu137–Asp144) and $\beta4$ (Tyr147–Ala154). Finally, the N- and C-terminal β-strands, $\beta1$ and $\beta4$, are parallel. The $\beta1$ and $\beta2$ strands are linked by a five-residue turn (Phe103–Ser107) showing strong sequential d_{NN} connectivities from Ala104 to Ser107. A four-residue turn (Asp144–Tyr147) connects the other pair of antiparallel strands, $\beta3$ and $\beta4$. The strong $d_{NN}(145,146)$ suggests a type I turn. The NH exchange rates indicate that the N- and C-terminal strands are nonperipheral. The two outer strands, on the other hand, show exchange patterns characteristic for peripheral strands (Figure 3). Furthermore, the $^3J_{NH\alpha}$ coupling constants are, as expected, high (>8 Hz) (Wüthrich, 1986) for the majority of the residues involved in the β-sheet.

The observation of $d_{NN}(i, i + 1)$, $d_{\alpha N}(i, i + 3)$, $d_{\alpha N}(i, i + 4)$, and $d_{\alpha\beta}(i, i + 3)$ connectivities, slow amide proton exchange, and small $^3J_{HN\alpha}$ coupling constants (<5 Hz) shows the existence of an α-helix in the region Phe117–Leu131. Two loops connect the N- and C-terminus of the helix to the second and third β-strands, respectively.

Global Fold. The secondary structure of the protein L domain involves both α-helical and β-sheet structures. The distribution of polar and nonpolar side chains on both the helix and the sheet are highly asymmetric. From a helical-wheel projection of the residues involved in the helix, one finds a nonpolar side created by the side chains of Phe117, Ala120, Ala124, Tyr127, Ala128, and Leu131. Also, the sheet is amphiphilic, with, for instance, the side chains of Val95, Ile97, Ala99, Leu101, Phe103, Tyr147, Leu149, Ile151, and Phe153 from the two inner β-strands forming a hydrophobic surface. The formation of a hydrophobic core by those surfaces is supported by a number of long-range NOEs observed between the nonpolar sides of the sheet and the helix. For example, the δCH_3 protons of Leu131 in the helix show cross peaks to the aromatic protons of Phe103 and Phe153 in the sheet. The aromatic protons of Phe117 show connectivities to the aromatic protons of Tyr147 and to the δCH_3 protons of Ile97. NOEs are also found between the δCH_3 protons of Ile151 and the βCH_3 protons of Ala124. These contacts confirm that a hydrophobic interior is created by the nonpolar side chains and allows us to make a schematic diagram of the fold for the B1 domain of protein L (Figure 5).

DISCUSSION

This work has shown that the Ig light chain-binding domain of protein L adopts a well-defined structure in solution. The domain contains a short disordered N-terminus followed by a folded unit comprising a four-stranded β-sheet with a central α-helix crossing over. A similar tertiary organization is to be expected for the other four Ig-binding domains due to the high degree of homology between the B domains (70–80% sequence homology at both the amino acid and nucleotide level). As previously stated, the N- and C-terminal strands of the B1 domain, $\beta1$ and $\beta4$, forms a parallel pair of strands, which places the N- and C-termini on opposite sides of the domain. The five B domains can therefore be connected to each other in a linear arragement in the native protein, as pearls on a string. This is in agreement with the observation that protein L is a fibrous, elongated molecule (Akerström & Björck, 1989).

The structure of the folded unit of the protein L domain is similar to that of the IgG Fc-binding domains of streptococcal protein G (Lian et al., 1991; Gronenborn et al., 1991; Orban et al., 1992). The structural similarities between the IgG-binding domains of protein G and human ubiquitin has previously been reported (Kraulis, 1991). Protein G contains Fc-binding domains of 55 amino acid residues which are linked by smaller repeats of 15 amino acids. The folded unit of the

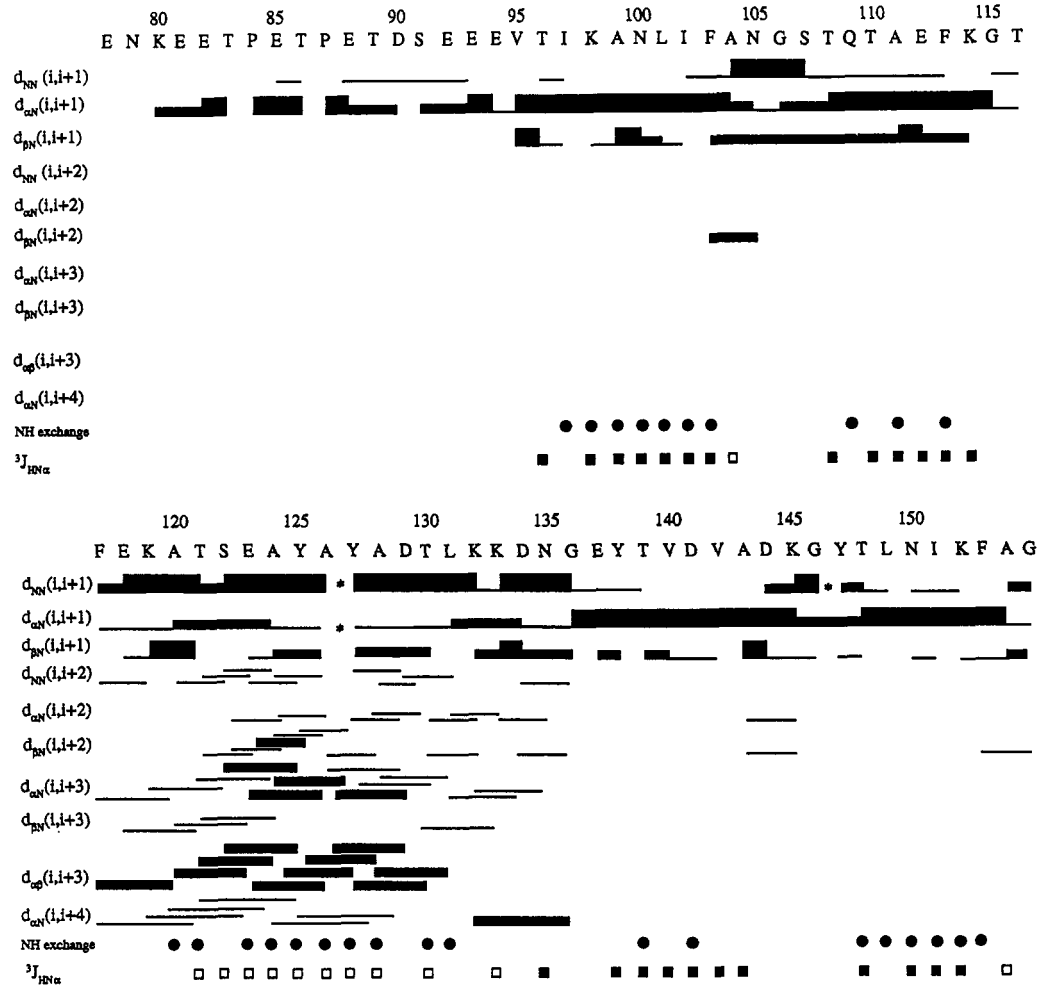

FIGURE 3: Summary of sequential and medium-range NOE connectivities, slowly exchanging amide protons, and $^3J_{HN\alpha}$ coupling constants for the B1 domain. The height of the bars gives a qualitative measure of the strength of the NOEs, classified as strong, medium, or weak. Connectivities that could not be observed due to degeneracy are marked with an asterisk. Amide protons that did not exchange with D_2O after 15 h at 27 °C, pH 5.0, are marked (●). Values of $^3J_{HN}$ are summarized as $^3J_{HN\alpha} < 5$ Hz (□) and $^3J_{HN\alpha} > 8$ Hz (■).

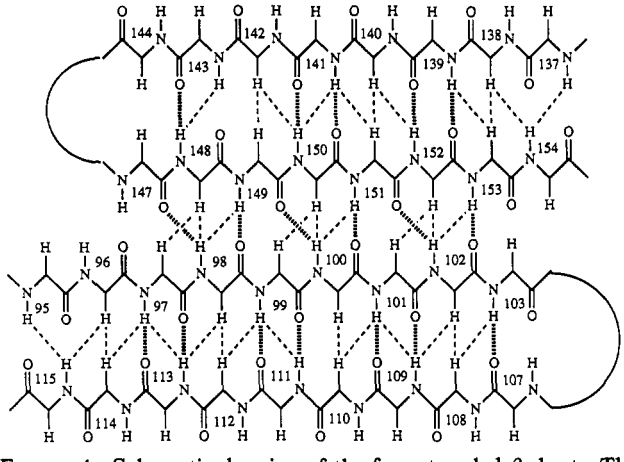

FIGURE 4: Schematic drawing of the four-stranded β-sheet. The two inner β-strands are parallel, whereas the two outer pairs of β-strands are antiparallel. NOE connectivities between the backbone protons are represented by dashed lines. Hydrogen bonds, indicated by hatched lines, are drawn on the basis of the observation of slowly exchanging amide protons.

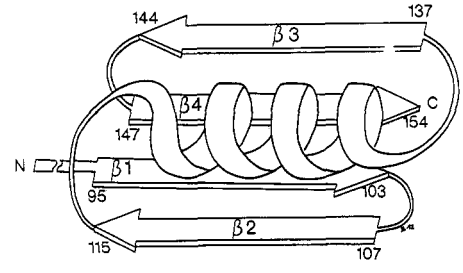

FIGURE 5: Schematic representation of the tertiary organization for the B1 domain of protein L.

protein L domain consists of 61 amino acid residues, which makes it comparable to the size of a protein G domain. This folded unit is preceded by a 15 amino acid long disordered N-terminus which is present in all five domains. Those disordered segments connecting the five Ig binding domains may facilitate the interaction with Ig light chains by increasing the individual flexibility of the domains. Another characteristic shared between protein L and protein G is that both are stable to thermal denaturation, although neither protein contains any disulfide bridges. Differential scanning calorimetry has been applied to two of the protein G domains (Alexander et al., 1992) and the melting temperatures were found to be 87.5 and 79.4 °C. The corresponding T_m for the protein L B1 domain is 76.5 °C at pH 6.0 (P. Sellers, unpublished experiments). Important factors contributing to the thermal stability of the two proteins are probably the large number of hydrogen bonds in the secondary structures and the hydrophobic interaction between residues in the interface between the nonpolar sides of the helix and the sheet.

The structural similarities between protein G and protein L described here were unexpected since the DNA sequences encoding the Ig-binding protein G and protein L domains share no significant degree of homology, and the gene products show affinity for different sites on Ig: protein G for the Cγ2–Cγ3 interface region of IgG (Stone et al., 1989) and protein

L for the framework region on the variable domain of κ light chains (Nilson et al., 1992). Protein G and two additional IgG Fc-binding bacterial proteins, protein A of *S. aureus* (Forsgren & Sjöquist, 1966) and protein H of group A streptococci (Akesson et al., 1990), were recently found to bind to closely located or even overlapping regions on IgG Fc (Frick et al., 1992), although their Fc-binding regions are nonrelated at the primary structural level. Furthermore, the secondary structure of an Fc-binding protein A domain is significantly different from the structure of a corresponding protein G domain. An Fc-binding domain of protein A is, in solution, composed of three consecutive helices packed together (Torigoe et al., 1990), demonstrating that in the case of protein A and protein G different structures bind to closely related sites, whereas in the case of protein G and protein L similar folds are used to bind to different sites in the Ig molecule. These observations emphasize the structural complexity of protein–protein interactions and the need for a further three-dimensional structural analysis of proteins L and G alone and of the complexes between these proteins and Ig light chains and IgG Fc fragments, respectively.

P. magnus bacteria are normally found on most body surfaces, where they are members of the indigenous flora. The bacteria are, however, also causative agents in a variety of infections (Sutter et al., 1985). Only about 10% of *P. magnus* strains have the protein L gene, and these strains are more frequently connected with clinical infections (Kastern et al., 1990), suggesting that protein L is a virulence determinant. This is in contrast to protein G, which is equally expressed in group C and G streptococci strains that have been isolated from patients with severe clinical infections or from healthy carriers (Sjöbring et al., 1989). A possible explanation for this difference could be that Ig bound to protein L or protein G at the bacterial surface, is exposed differently. An antibody molecule bound to protein L through light chain interactions can bind to Fc receptors on host cells, whereas the Fc region of IgG antibodies bound to protein G is blocked. Moreover, protein L-expressing peptostreptococci can bind all classes of Ig. For instance, such a bacterium, or protein L itself, is capable of inducing histamine release from human basophils and mast cells by binding to and cross-linking surface IgE (Patella et al., 1990). Therefore, from a functional point of view, the protein L and G domains seem to play different roles, regardless of their common structural organization. Keeping in mind that the host–parasite relationship represents a delicate balance between multiple molecular events and that virulence is a highly polygenic property, this is not surprising. However, if the fold of the Ig-binding domains of protein L and G were to be found in other proteins, this could shed light on the evolution and function of this structural unit.

ACKNOWLEDGMENT

We are indebted to Ingbritt Gustafsson for invaluable technical assistance, Mikael Akke, Charlotta Johansson, and Bryan Finn for helpful discussions, and Peter Drakenberg for the use of the MAGNE program.

REFERENCES

Alder, M., & Wagner, G. (1991) *J. Magn. Reson. 91*, 450–454.
Akerström, B., & Björck, L. (1989) *J. Biol. Chem. 267*, 19740–19746.
Akesson, P., Cooney, J., Kishimodo, F., & Björck, L. (1990) *Mol. Immunol. 27*, 523–531.
Alexander, P., Fahnestock, S., Lee, T., Orban, J., & Bryan, P. (1992) *Biochemistry 31*, 3597–3603.
Aue, W. P., Batholdi, E., & Ernst, R. R. (1976) *J. Chem. Phys. 64*, 2229–2246.
Bax, A. (1985) *J. Magn. Reson. 65*, 142–145.
Bax, A., & Davis, D. G. (1985) *J. Magn. Reson. 65*, 355–360.
Billeter, M., Braun, W., & Wüthrich, K. (1982) *J. Mol. Biol. 155*, 321–346.
Björck, L. (1988) *J. Immunol. 140*, 1194–1197.
Björck, L., & Kronvall, G. (1984) *J. Immunol. 133*, 969–974.
Boyle, M. D. P., Ed. (1990) *Bacterial Immunoglobulin Binding Proteins*, Vol. I, Academic Press, San Diego, CA.
Braunschweiler, L., & Ernst, R. R. (1983) *J. Magn. Reson. 53*, 521–528.
Braunschweiler, L., Bodenhausen, G., & Ernst, R. R. (1983) *Mol. Phys. 48*, 535–560.
Chazin, W. J., Rance, M., & Wright, P. E. (1988) *J. Mol. Biol. 202*, 603-622.
Dalböge, H., Bech Jensen, E., Töttrup, H., Grubb, A., Abrahamson, M., Olafsson, I., & Carlsen, S. (1989) *Gene 79*, 325–332.
Forsgren, A., & Sjöquist, J. (1966) *J. Immunol. 97*, 822–827.
Frick, I.-M., Wikström, M., Forsén, S., Drakenberg, T., Gomi, H., Sjöbring, U., & Björck, L. (1992) *Proc. Natl. Acad. Sci. U.S.A. 89*, 8532–8536.
Gronenborn, A. M., Filpula, D. R., Essig, N. Z., Achari, A., Whitlow, M., Wingfield, P. T., & Clore, G. M. (1991) *Science 254*, 657–661.
Kastern, W., Holst, E., Nielsen, E., Sjöbring, U., & Björck, L. (1990) *Infect. Immunol. 58*, 1217–1222.
Kastern, W., Sjöbring, U., & Björck, L. (1992) *J. Biol. Chem. 267*, 12820–12825.
Kraulis, P. J. (1991) *Science 254*, 581–582.
Levitt, M., & Freeman, R. (1979) *J. Magn. Reson. 33*, 473–476.
Lian, L.-Y., Yang, J. C., Derrick, J. P., Sutcliffe, M. J., Roberts, G. C. K., Murphy, J. P., Goward, C. R., & Atkinson, T. (1991) *Biochemistry 30*, 5335–5340.
Macura, A., & Ernst, R. R. (1980) *Mol. Phys. 41*, 95–117.
Myhre, E. B., & Erntell, M. (1985) *Mol. Immunol. 22*, 879–885.
Nilson, B. H. K., Solomon, A., Björck, L., & Akerström, B. (1992) *J. Biol. Chem. 267*, 2234–2239.
Orban, J., Alexander, P., & Bryan, P. (1992) *Biochemistry 31*, 3604–3611.
Patella, V., Casolaro, V., Björck, L., & Marone, G. (1990) *J. Immunol. 145*, 3054–3061.
Rance, M. (1987) *J. Magn. Reson. 74*, 557–564.
Rance, M., Sorensen, O. W., Bodenhausen, G., Wagner, G., Ernst, R. R., & Wüthrich, K. (1983) *Biochem. Biophys. Res. Commun. 131*, 1094–1102.
Reis, K. J., Ayoub, E. M., & Boyle, M. D. P. (1984) *J. Immunol. 132*, 3091–3097.
Shaka, A. J., Lee, C. J., & Pines, A. (1988) *J. Magn. Reson. 77*, 274–293.
Sjöbring, U., Björck, L., & Kastern, W. (1989) *Mol. Microbiol. 3*, 3054–3061.
States, D. J., Haberkorn, R. A., & Ruben, D. J. (1982) *J. Magn. Reson. 48*, 286–292.
Stone, C. G., Sjöbring, U., Björck, L., Sjöquist, J., Barber, C. V., & Nardella, F. A. (1989) *J. Immunol. 143*, 565–570.
Sutter, V., Citron, D., Edelstein, M., & Finegold, S. (1985) *Wadsworth Anareobic Bacteriology Manual*, 4th ed., VA Wadsworth Medical Center, University of California, Los Angeles, CA.
Torigoe, H., Shimada, I., Saito, A., Sato, M., & Arata, Y. (1990) *Biochemistry 29*, 8787–8793.
Wagner, G. (1983) *J. Magn. Reson. 55*, 151–156.
Wüthrich, K. (1986) *NMR of Proteins and Nucleic Acids*, Wiley, New York.